SUNY Geneseo
KnightScholar

Psychology faculty/staff works | By Department

2009

Mutation I810N in the α3 isoform of Na+,K +-ATPase causes impairments in the sodium pump and hyperexcitability in the CNS

Steven J. Clapcote

Steven Duffy

Gang Xie

Greer Kirshenbaum

Allison R. Bechard
SUNY Geneseo

See next page for additional authors

Follow this and additional works at: https://knightscholar.geneseo.edu/psychology-faculty

Recommended Citation

Clapcote S.J., Duffy S., Xie G., Kirshenbaum G., Bechard A.R., Schack V.R., Petersen J., Sinai L., Saab B.J., Lerch J.P., Minassian B.A., Ackerley C.A., Sled J.G., Cortez M.A., Henderson J.T., Vilsen B., Roder J.C. (2009). Proceedings of the National Academy of Sciences of the United States of America, 106, 14085-14090 doi: 10.1073/pnas.0904817106

This Article is brought to you for free and open access by the By Department at KnightScholar. It has been accepted for inclusion in Psychology faculty/staff works by an authorized administrator of KnightScholar. For more information, please contact KnightScholar@geneseo.edu.

Authors

Steven J. Clapcote, Steven Duffy, Gang Xie, Greer Kirshenbaum, Allison R. Bechard, Vivien Rodacker Schack, Janne Petersen, Laleh Sinai, Bechara J. Saab, Jason P. Lerch, Berge A. Minassian, Cameron A. Ackerley, John G. Sled, Miguel A. Cortez, Jeffrey T. Henderson, Bente Vilsen, and John C. Roder

This article is available at KnightScholar: https://knightscholar.geneseo.edu/psychology-faculty/2

PNAS PNAS PNAS PNAS

Mutation I810N in the α3 isoform of Na^+,K^+-ATPase causes impairments in the sodium pump and hyperexcitability in the CNS

Steven J. Clapcote[a,b,1], Steven Duffy[a], Gang Xie[a], Greer Kirshenbaum[a,c], Allison R. Bechard[a], Vivien Rodacker Schack[d], Janne Petersen[d], Laleh Sinai[a,c], Bechara J. Saab[a,c], Jason P. Lerch[e], Berge A. Minassian[c,e], Cameron A. Ackerley[e], John G. Sled[c,e], Miguel A. Cortez[c,e], Jeffrey T. Henderson[c], Bente Vilsen[d], and John C. Roder[a,c]

[a]Samuel Lunenfeld Research Institute, Mount Sinai Hospital, Toronto, ON, Canada M5G 1X5; [b]Institute of Membrane and Systems Biology, University of Leeds, Leeds LS2 9JT, United Kingdom; [c]Departments of Medical Biophysics, Medical Genetics, Paediatrics, and Pharmaceutical Sciences, University of Toronto, Toronto, ON, Canada M5S 1A1; [d]Department of Physiology and Biophysics, Centre for Membrane Pumps in Cells and Disease–PUMPKIN, Danish National Research Foundation, University of Aarhus, DK-8000 Aarhus, Denmark; and [e]Mouse Imaging Centre, Program in Genetics and Genome Biology, and Divisions of Neurology and Pathology, Hospital for Sick Children, Toronto, ON, Canada M5G 1X8

Edited by Ernest Marshal Wright, University of California, Los Angeles, CA, and accepted by the Editorial Board June 9, 2009 (received for review May 1, 2009)

In a mouse mutagenesis screen, we isolated a mutant, *Myshkin* (*Myk*), with autosomal dominant complex partial and secondarily generalized seizures, a greatly reduced threshold for hippocampal seizures in vitro, posttetanic hyperexcitability of the CA3-CA1 hippocampal pathway, and neuronal degeneration in the hippocampus. Positional cloning and functional analysis revealed that *Myk*/+ mice carry a mutation (I810N) which renders the normally expressed Na^+,K^+-ATPase α3 isoform inactive. Total Na^+,K^+-ATPase activity was reduced by 42% in *Myk*/+ brain. The epilepsy in *Myk*/+ mice and in vitro hyperexcitability could be prevented by delivery of additional copies of wild-type Na^+,K^+-ATPase α3 by transgenesis, which also rescued Na^+,K^+-ATPase activity. Our findings reveal the functional significance of the Na^+,K^+-ATPase α3 isoform in the control of epileptiform activity and seizure behavior.

alpha3 Na^+,K^+ ATPase | BAC rescue | epilepsy | forward genetic screen | mouse

Epilepsy is a debilitating neurological disorder characterized by recurrent seizures triggered by excessive neuronal excitability in the brain. At least 40–50% of all forms of epilepsy are idiopathic, and thus have a presumed genetic origin (1). Identifying genetic and pathophysiological pathways involved in epilepsy is critical for the rational design of improved treatments for the one-third of epilepsy patients who do not respond to current medications (2).

Na^+,K^+-ATPases (sodium/potassium pumps) play a seminal role in controlling neuronal excitability by maintaining electrochemical gradients for Na^+ and K^+ across the plasma membrane. Hence, it has been hypothesized that an abnormality in Na^+,K^+-ATPase could facilitate seizures (3–6). Indeed, partial inhibition of Na^+,K^+-ATPase activity with cardiac glycosides has been shown to induce seizures in rats (7–9). Furthermore, some patients with the autosomal dominant genetic disorder familial hemiplegic migraine (FHM) type 2, caused by mutation of the Na^+,K^+-ATPase α2-isoform, have a clinical history of epileptic seizures (10). Three isoforms of the Na^+,K^+-ATPase α-subunit, α1, α2, and α3, encoded by paralogous genes (*Atp1a1*, *Atp1a2*, and *Atp1a3*, respectively), are expressed in mammalian brain: α1 as the housekeeping enzyme in a variety of cell types, α2 predominantly in glial cells in human adults, and α3 exclusively in neurons (11). The increased epileptic propensity observed in patients with FHM, and thus the role of the Na^+,K^+-ATPase α2-isoform in generation of seizures, has been explained by the reduced ability of glial cells to clear the extracellular space of K^+ and glutamate (6). So far there has been no convincing evidence linking the neuron specific α3-isoform of Na^+,K^+-ATPase to epilepsy. Mutations in the human *ATP1A3* gene encoding α3 are associated with rapid-onset dystonia-parkinsonism (RDP), but seizures are not a typical characteristic of this disease (12)—possibly because most known RDP mutations are compatible with partial NKA function (13). The similar affinities of α2 and α3 for the Na^+,K^+-ATPase inhibitor ouabain have precluded conclusive pharmacological studies of isoform specificity.

Here, we present a mouse model for epilepsy caused by mutation of the Na^+,K^+-ATPase α3-isoform. We have used in vivo mutagenesis with N-nitroso-N-ethylurea (ENU) (14) to generate a mutant named *Myshkin* (*Myk*) that displays seizures and neuronal hyperexcitability in heterozygotes (*Myk*/+) and perinatal death in homozygotes (*Myk*/*Myk*). The *Myshkin* allele contains a point mutation in the Na^+,K^+-ATPase α3-isoform that inactivates this enzyme and is solely responsible for complex partial and secondarily generalized seizures in these mice.

Results and Discussion

In a screen for dominant visible phenotypes among 8-week-old progeny of ENU mutagenized 129S1/SvImJ (129S1) males and untreated C57BL/6J females, we found a female with a small body. This phenotype proved to be heritable as a Mendelian autosomal dominant trait, as 10 of 23 (43.5%) N2 progeny of this mouse and a C57BL/6NCr (B6) male had a visibly smaller body than their same-sex littermates (see Fig. S1). We observed that the small mice exhibited spontaneous, recurrent convulsive seizures in the home cage from weaning at 4 weeks of age. When bred to homozygosity, *Myk*/*Myk* pups appeared grossly normal but died shortly after birth, indicating that the seizure and small body phenotype of *Myk*/+ mice is semidominant. We localized the *Myshkin* allele to a nonrecombinant interval of chromosome 7 (Fig. 1). Sequencing of genomic DNA and whole brain cDNA from *Myk*/*Myk* ($n = 2$), *Myk*/+ ($n = 2$), and +/+ ($n = 2$) mice revealed 2 de novo mutations in the *Atp1a3* gene encoding the α3 isoform of the Na^+,K^+-ATPase, predicted to result in amino acid substitutions Asp^{65}→Glu (D65E) and Ile^{810}→Asn (I810N) (Fig. 1). Each of these amino acids is conserved across vertebrate species (Fig. 1). Both mutations appeared in 107 *Myk*/+ mice after 12 generations of backcrossing to B6, but neither was found in 104 +/+ littermates. Hence, *Myshkin* is an allele of *Atp1a3* (*$Atp1a3^{Myk}$*).

NEUROSCIENCE

Author contributions: J.C.R. designed research; S.J.C., S.D., G.X., G.K., A.R.B., V.R.S., J.P., L.S., B.J.S., J.P.L., B.A.M., C.A.A., J.G.S., M.A.C., J.T.H., and B.V. performed research; S.J.C., S.D., G.K., A.R.B., V.R.S., J.P., L.S., B.J.S., J.P.L., B.A.M., C.A.A., J.G.S., M.A.C., J.T.H., B.V., and J.C.R. analyzed data; and S.J.C., S.D., B.V., and J.C.R. wrote the paper.

The authors declare no conflict of interest.

This article is a PNAS Direct Submission. E.M.W. is a guest editor invited by the Editorial Board.

[1]To whom correspondence should be addressed at: Institute of Membrane and Systems Biology, Garstang Building, University of Leeds, Leeds LS2 9JT, United Kingdom. E-mail: s.j.clapcote@leeds.ac.uk.

This article contains supporting information online at www.pnas.org/cgi/content/full/0904817106/DCSupplemental.

Fig. 1. Positional cloning of *Myshkin*. (*A*) Fine mapping of the *Myshkin* mutation on Chr 7. White squares represent 129S1:B6 heterozygous alleles and black squares represent homozygous B6 alleles. The number of progeny inheriting each haplotype is listed on the bottom line. (*B*) DNA sequence traces of *Atp1a3* exons 4 and 18 from *Myshkin* mice and the 129S1 and B6 parental strains. Asterisks indicate the location of a T→A transversion at nucleotide 328 and a T→A transversion at nucleotide 2,562. The sequences of *Atp1a3* exons 4 and 18 in the mapping strains 129S1 and B6 are identical, indicating that 328T→A and 2562 T→A are de novo mutations. (*C*) *Eco*O109I restriction site (5′-AG*GGCCT-3′) generated by the 328T→A mutation in *Atp1a3*. A 576-bp PCR amplicon is cleaved by *Eco*O109I into 212-bp and 354-bp fragments. (*D*) Alignment of partial $\alpha 3$ protein sequences of several vertebrate species (*Upper*) and partial *Mus musculus* $\alpha 1$, $\alpha 2$, and $\alpha 3$ protein sequences *(Lower)*, showing conservation of amino acids D65 (Blue text) and I810 (Red text).

The functional characteristics of mutations D65E and I810N of the Na^+,K^+-ATPase have not previously been studied in vitro or in vivo. The double mutant D65E+I810N and each point mutant D65E and I810N were examined by transfecting COS cells (15). Each mutant was expressed to a wild type-like level and targeted normally to the plasma membrane (Fig. S2). The Na^+,K^+-ATPase activities of the D65E+I810N and I810N $\alpha 3$ mutants, but not D65E, were too low to support growth and survival of COS cells. Thus, I810N alone disrupts enzyme function. D65E $\alpha 3$ exhibited unimpaired function with normal catalytic turnover rate and Na^+, K^+, and ATP affinities (Fig. S2). Asp^{65} is located at the cytosolic NH_2 terminus, whereas Ile^{810} is located in the membrane (16), where it may interact with Thr^{329} (Fig. S3). Disruption of this interaction by introducing the polar asparagine at position 810 might destabilize the ion binding pocket, which is constituted by oxygen containing residues close to Ile^{810} (16).

Weaned *Myk*/+ mice exhibited spontaneous, recurrent behavioral convulsions in the home cage (Fig. 2), which could also be evoked reliably by vestibular stress. Seizures started with running and leaping, behavioral arrest (freezing/staring), and Straub tail, followed by whole body clonic jerking and falling, resembling partial complex seizures with secondary generalization (localized attack preceding whole body convulsions). Seizures were accompanied by salivation, and occasionally progressed to maximal tonic hindlimb extension, which was invariably followed by death (Movie S1).

We observed freely moving *Myk*/+ ($n = 9$) and +/+ ($n = 6$) mice for 30–45 min by synchronous video monitoring and electrocorticographic (ECoG) recordings. Spontaneous behavioral seizures were accompanied by classical neocortical and depth amygdala spike-and-waves characteristic of epileptic discharges. In *Myk*/+ mice, rhythmic vertical shaking of the cage (vestibular stress) induced intermittent sharp waves (preictal) that increased in amplitude until generalized bilaterally synchronous tonic-clonic seizure activity was observed (ictal), whereas no such seizure activity was observed in +/+ mice (Fig. 2). In 3 of 9 *Myk*/+ mice, the cage shaking induced convulsive seizures immediately (Movie S2).

Treatment with valproic acid (VPA), a broad spectrum antiepileptic drug, reduced the severity of seizures exhibited by *Myk*/+ mice after cage shaking (VPA: 0.69 ± 0.41, Vehicle: 2.4 ± 0.70; $F_{(1, 22)} = 4.86$, $P = 0.039$; 1–6 scale). Moreover, epilepsy in *Myk*/+ mice could be prevented by delivery of additional copies of wild-type Na^+,K^+-ATPase $\alpha 3$ by transgenesis with a bacterial artificial chromosome (BAC) containing *Atp1a3* and its promoter. BAC transgenic mice showing a $58 \pm 6\%$ increase in $\alpha 3$ protein level in the brain (Fig. S4) were crossed with *Myk*/+ mice to yield *Myk*/+/BAC mice. Cage shaking did not induce seizures in *Myk*/+/BAC

Fig. 2. Epileptic seizures in *Myk*/+ mice. (*A*) Spontaneous seizure in 16-week-old *Myk*/+ N2 B6 male. Frames 1–4 were captured at 4-s intervals after the loss of postural control. (*B*) Electrocorticogram trace from *Myk*/+ mouse before (Preinduction) and after cage shaking (Postinduction). (*C*) Number of electrographic seizures observed in +/+ ($n = 6$), *Myk*/+ ($n = 9$, **, $P < 0.005$), and *Myk*/+/BAC ($n = 6$) mice after cage shaking.

mice during ECoG recordings (Fig. 2), and no behavioral signs of seizures after ECoG testing, nor mortality within 2 weeks, were observed. In contrast, 5 of 6 *Myk*/+ littermates subjected to the same treatment showed convulsive seizures and epileptiform discharges.

Combined hippocampus-entorhinal cortex slices (Fig. 3) are useful for investigation of the mechanisms of seizure induction and spread in the medial temporal lobe (17). Superfusion of Mg^{2+}-free artificial cerebrospinal fluid, a treatment that over-activates NMDA receptors (18), induced repeated synchronized ictal bursts in CA3 and the entorhinal cortex (EC) in more than half of the slices from *Myk*/+ mice, whereas such bursts were only rarely observed in +/+ slices (Fig. 3). The remaining *Myk*/+ slices exhibited only brief asynchronous interictal bursts (CA3) and negative DC shifts (EC) similar to those characteristic of +/+ slices, but the epileptiform activity appeared sooner after Mg^{2+} removal in *Myk*/+ slices than in +/+ slices (Fig. 3). The enhanced epileptic propensity of hippocampal-EC slices from *Myk*/+ mice was rescued by BAC transgenesis of additional copies of wild-type Na^+,K^+-ATPase $\alpha3$ (Fig. 3).

Hippocampal slices from *Myk*/+ mice showed enhanced excitation-spike (E-S) coupling after theta burst stimulation (TBS), as determined by the relation between the postsynaptic population action potential (popAP) spike and the field excitatory postsynaptic potential (fEPSP) (Fig. 4), indicating that the CA3–CA1 hippocampal pathway became hyperexcitable after physiological patterns of high-frequency synaptic activity. Under basal conditions, this pathway had wild type-like synaptic transmission, plasticity, and excitability (Fig. S5). Over-stimulation of NMDA receptors induces seizures (18, 19), and the observed posttetanic increase in E-S coupling in CA1 pyramidal neurons may result from an NMDA receptor-dependent long-term depression (LTD) of feed-forward $GABA_A$-mediated inhibition (19).

The neuropathology of young adult *Myk*/+ mice showed histological sequela of seizures, such as medial temporal sclerosis and aberrant membranous whorls in hippocampal pyramidal neurons in CA3 and CA1 (see *SI Text*, Fig. S6).

The total specific Na^+,K^+-ATPase activity of brain homogenates (contributed by $\alpha1$, $\alpha2$, and $\alpha3$ isoforms) showed a reduction by $42 \pm 3\%$ in 10-week-old *Myk*/+ mice relative to their +/+ littermates, whereas the rescued *Myk*/+/BAC mice showed significantly less reduction ($26 \pm 3\%$) (Fig. 5). Neither the Na^+,K^+-ATPase activity per active catalytic site [*Myk*/+:$7{,}142 \pm 349$ min^{-1} ($n = 15$) versus +/+:$7{,}776 \pm 309$ min^{-1} ($n = 12$)] nor the affinities for Na^+ and K^+ were significantly different between *Myk*/+ and +/+ mice (Fig. S7), suggesting that the residual 58% activity in *Myk*/+ brain is derived from the normal $\alpha3$ enzyme encoded by the wild-type allele. The near halving of Na^+,K^+-ATPase activity in *Myk*/+ mice indicates that $\alpha3$ is the functionally dominant Na^+,K^+-ATPase α isoform in the young adult brain. In contrast, total brain Na^+,K^+-ATPase activity in E18 fetuses was $44 \pm 3\%$ in *Myk*/*Myk* and $66 \pm 5\%$ in *Myk*/+ relative to +/+ littermates (Fig. 5), indicating more significant contributions from $\alpha1$ and $\alpha2$ during development. No functional phosphorylatable $\alpha3$ Na^+,K^+-ATPase enzyme was expressed in the brains of *Myk*/*Myk* fetuses, as indicated by the lack of Na^+,K^+-ATPase phosphorylation from [γ-^{32}P]ATP in brain homogenates under high Mg^{2+} conditions where the phosphorylation of $\alpha2$ is negligible (Fig. S7). Western blot analysis did not reveal differences in $\alpha3$ protein abundance in whole brain from *Myk*/*Myk* and *Myk*/+ fetuses or *Myk*/+ adults (Fig. 5), and immunocytochemical analysis of cultured neocortical neurons demonstrated normal membrane targeting of $\alpha3$ over the surface of the soma and processes and colocalization with agrin (Fig. 5), an endogenous $\alpha3$ inhibitor that enhances membrane depolarization and increases action potential frequency in cortical neurons (20). Thus, *Myshkin* is functionally a null allele of *Atp1a3* that encodes a normally expressed, but inactive enzyme.

To further establish a causal link between the *Myshkin* mutation and the observed phenotype, we performed a complementation test for recessive perinatal lethality. Heterozygous *Myshkin* males were crossed with female mice heterozygous for a point mutation in *Atp1a3* intron 4 (*Atp1a3^{tm1Ling}*) that show reduced $\alpha3$ expression (21). No *tm1Ling*/*Myk* mice were detected among the 128 progeny at 4 weeks of age. These results, together with the rescue of the epileptic phenotype in the *Myk*/+/BAC mice (Figs. 2 and 3), indicate that the *Myshkin* mutation is solely responsible for the epileptic phenotype. Hence, we have shown that a loss-of-function mutation of $\alpha3$ Na^+,K^+-ATPase causes epilepsy in mice. In contrast, seizures were not reported in *Atp1a3$^{tm1Ling/+}$* mice, even on the relatively seizure-prone Black Swiss background (21, 22) rather

Fig. 3. Reduced threshold for epileptiform activity in *Myk*/+ mice. (*A*) Bright-field image of transverse slice of hippocampus and entorhinal cortex (EC). Positions of the stimulating electrode (S) and of the recording electrodes (R) are illustrated. (*B*) Time to start of quasi rhythmic spiking after washout of extracellular Mg^{2+} (*, $P < 0.05$, **, $P < 0.005$, *t* test). (*C*) Response incidence for different types of epileptiform activity (illustrated in *D* and *E*) within 1 h of Mg^{2+} washout. "Sync" refers to the incidence of synchronized ictal bursts in EC and CA3 within 2 h of Mg^{2+} washout (**, $P < 0.005$, χ^2-test). (*D*) Sample sweeps illustrating repeating synchronized ictal bursts in *Myk*/+ slice. Below is shown a single ictal burst on an expanded time scale. (*E*) Typical sample sweeps from +/+ slice.

than the seizure-resistant B6 strain of *Myshkin* (23). However, 10-week-old *tm1Ling*/+ mice displayed only a 16 ± 4% reduction in brain Na^+,K^+-ATPase activity, which is even less than the modest reduction in seizure-resistant *Myk*/+/BAC mice (Fig. 5). The *tm1Ling*/+ mice showed a greatly reduced expression of the pore forming NR1 subunit of the NMDA receptor (21), whilst expression in *Myk*/+ mice was unaltered relative to +/+ littermates (Fig. 5). Chronic over-stimulation of NMDA receptors is known to induce seizures (18, 19). Hence, synergism between $\alpha3$ Na^+,K^+-ATPase and NMDA receptor activities may contribute to determine the epileptic propensity, possibly through disruption of calcium metabolism.

There are several possibilities for explaining the observed link between dysfunction of the neuronal $\alpha3$-isoform of Na^+,K^+-ATPase and hyperexcitability. The loss of $\alpha3$ Na^+,K^+-ATPase activity might induce neuronal membrane depolarization accompanied by hyperexcitability through an increase of the extracellular K^+ concentration because of the deficient clearance by the Na^+,K^+-pump (4, 5). Although the $\alpha2$-isoform of Na^+,K^+-ATPase present in glial cells has been promoted as the major isoform involved in K^+ clearance, there are indications that neuronal Na^+,K^+-ATPase could be more important than glial Na^+,K^+-ATPase for K^+ clearance after epileptiform activity induced in hippocampal slices (8). Our finding that $\alpha3$ is the functionally dominant α subunit in the adult brain is consistent with the reported lack of seizures in $\alpha1$ or $\alpha2$ heterozygous mice (21, 24). Reduced $\alpha3$-mediated Na^+ transport in neurons might furthermore lead to a greater elevation in posttetanic intracellular Na^+ with a concomitant reduction in Na^+/Ca^{2+} exchanger-mediated calcium extrusion, and dysregulated calcium transients could lead to a rise of the intracellular Ca^{2+} level with accumulation of glutamate in the synaptic cleft (6) and to over-activation of calcineurin and internalization of GABA receptors (25, 26).

Conclusion

We have characterized a mutation I810N that inactivates the neuron-specific $\alpha3$-isoform of Na^+,K^+-ATPase and causes epilepsy in mice. Because of the importance of ion homeostasis in maintaining normal excitability, it is not surprising that Na^+,K^+-ATPase function is implicated in the development of epileptiform activity. Nevertheless, our study of mice with specific inactivation of the $\alpha3$ isoform reveals the functional significance of the $\alpha3$ isoform in the

Fig. 4. Enhanced E-S coupling (popAP:fEPSP ratio) in *Myk*/+ mice, 25–55 min after TBS. (*A*) Before TBS, the relation between the postsynaptic fEPSP slope in CA1 stratum radiatum and the popAP, measured at the same transverse location in CA1 stratum pyramidal, did not differ between genotypes (''baseline'', open symbols). After TBS, *Myk*/+ mice exhibited a higher E-S coupling (popAP:fEPSP slope) than +/+ mice. (*B*) Summary of the E-S coupling data in *A* (*, $P < 0.001$, **, $P < 10–9$, #$P < 0.01$).

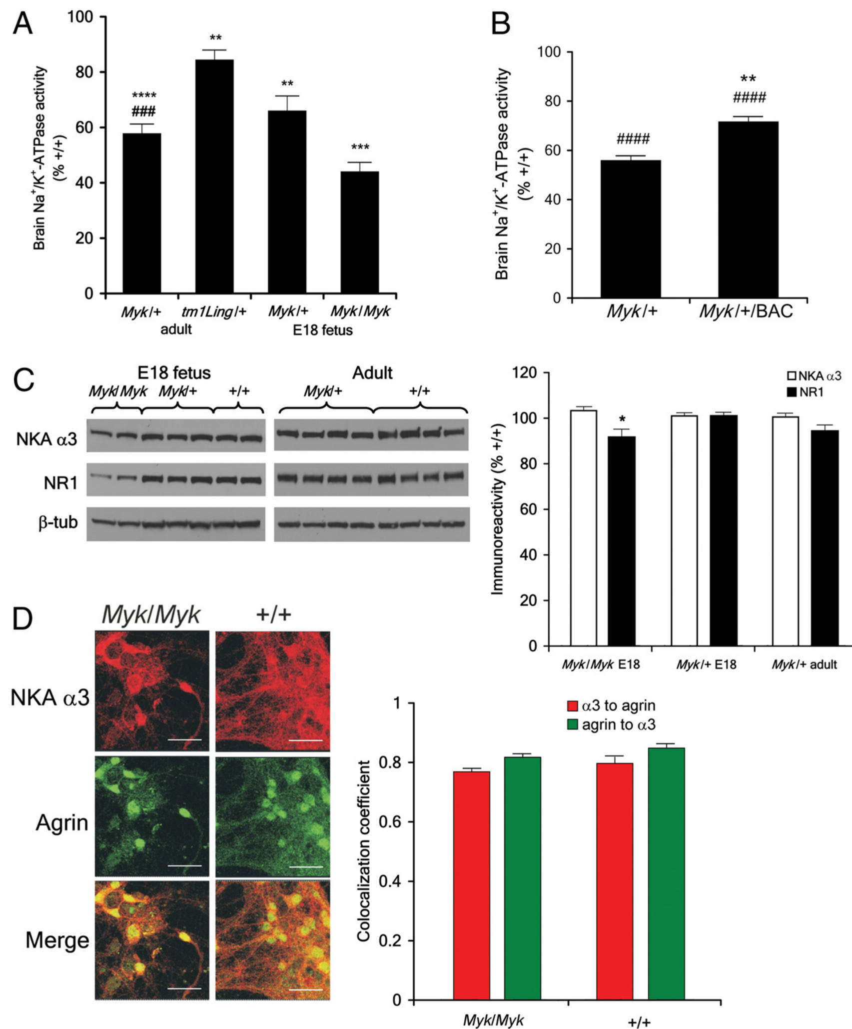

Fig. 5. Mutational and BAC transgenesis effects on Na$^+$,K$^+$-ATPase activity and α3 expression in brain. (*A*) Specific Na$^+$,K$^+$-ATPase activity in brain homogenates of 10-week-old *Myk*/+ ($n = 6$) and *tm1Ling*/+ mice ($n = 4$) and of *Myk*/+ ($n = 11$) and *Myk*/*Myk* E18 fetuses ($n = 5$) (mean ± SEM). Results are expressed as a % of +/+ littermate levels (adults $n = 6$, fetuses $n = 7$). **, $P < 0.01$; ***, $P < 0.001$; ****, $P < 0.0001$ versus respective +/+ littermates; ###$P < 0.001$ versus *tm1Ling*/+ mice. (*B*) Specific Na$^+$,K$^+$-ATPase activity in brain homogenates of 10-week-old *Myk*/+ ($n = 4$) and *Myk*/+/BAC ($n = 4$) mice (mean ± SEM). Results are expressed as a % of +/+ littermate levels. **, $P < 0.01$ versus *Myk*/+ mice; ####$P < 0.0001$ versus +/+ mice. (*C*) Typical blots of 20 μg protein from brains probed with anti- Na$^+$,K$^+$-ATPase α3, anti-NR1, and anti-β-tubulin III antibodies (*Left*). Immunoreactivity of *Myk*/*Myk* ($n = 4$) and *Myk*/+ ($n = 6$) E18 fetus brains and *Myk*/+ ($n = 8$) adult brains expressed as a percentage of +/+ (E18 $n = 4$; adult $n = 8$) levels (*Right*). Each sample was blotted 3 times, and β-tubulin III was used as loading control. *, $P < 0.05$ versus +/+ E18 fetus brains (*Right*). (*D*) Distribution and signal intensity of α3 (Red) and agrin (Green) in cultured neocortical neurons from E18 fetuses (*Left*). (Scale bar, 24 μm.) Colocalization coefficients for *Myk*/*Myk* ($n = 14$) and +/+ ($n = 14$) E18 fetuses (*Right*).

control of epileptogenesis and seizure behavior. Given the high level of homology between the different Na$^+$,K$^+$-ATPase isoforms of mice and humans, our findings suggest that inactivating mutation of *ATP1A3* is a candidate mechanism for human epilepsy, and highlight α3 and its physiological regulators as putative targets for the rational design of antiepileptic therapies.

Materials and Methods

Mice. Animal procedures were approved by the Animal Management Committee of Mount Sinai Hospital and were conducted in accordance with the requirements of the Ontario Animals for Research Act 1971 and the Canadian Council on Animal Care. We backcrossed *Myk*/+ mice to the C57BL/6NCr strain (National Cancer Institute) for 12 generations before conducting phenotypic tests on sex-balanced groups of *Myk*/+ and +/+ N12 littermates at 10–14 weeks of age. PCR-based genotyping assays for each mouse line are described in the *SI Text*.

Linkage Mapping and Positional Cloning. The meiotic linkage mapping and positional cloning strategy that we used to identify the *Myshkin* mutation has been described previously (14).

Na$^+$,K$^+$-ATPase Mutants Expressed in COS Cells. Using the QuikChange Site-Directed Mutagenesis kit (Stratagene), mutations D65E, I810N, and the combination D65E+I810N were introduced directly into full-length cDNA encoding an ouabain resistant version of the human α3 isoform, which carried the mutations Q108R and N119D to reduce the affinity for ouabain (27). To examine the functionality of the mutant and wild-type ouabain resistant enzymes, the cDNAs inserted in the expression vector pCMV6-XL-5 were transfected into COS-1 cells grown in the presence of 5 μM ouabain, which preferentially inhibits the ouabain-sensitive Na$^+$,K$^+$-ATPase endogenously present in COS-1 cells (15).

Electrocorticography. Stereotactic implantation of electrodes and ECoG recordings were carried out on *Myk*/+, *Myk*/+/BAC, and +/+ mice, as described previously (28).

Valproic Acid Treatment and Seizure Scoring. From weaning at 4 weeks of age, *Myk*/+ mice were i.p. injected daily for 66 days with either sodium valproate (150 mg/kg; Sigma) dissolved in distilled water ($n = 13$) or vehicle ($n = 10$) in a volume of 10 mL/kg body weight. The dose was determined by reference to a previous study of C57BL/6 mice (29). Mice were placed in a clean cage 30 min after the last injection. After a habituation period of 5 min, the cage was shaken for 30 s and seizure behavior was observed for 2 min. Seizure behavior was quantified on a 1–6 scale using the following behavioral scoring system: 1, running; 2, staring; 3, tail raise/vibrating; 4, small myoclonic jerk; 5, large myoclonic jerk (raising mouse into the air); 6, tonic-clonic seizure. The score assigned reflected the highest grade seizure behavior expressed by the mouse within the test.

BAC Transgenic Mice. MSMg01–344N17 BAC DNA of *Mus musculus molossinus* origin was purified in a NucleoBond AX500 column (Machery-Nagel) and resuspended in polyamine microinjection buffer. BAC DNA was injected into the pronucleus of (C57BL/6 × SJL) F2 embryos, which were then transferred into the oviducts of 0.5 day pseudopregnant CD-1 females (Charles River Laboratories). From among the 154 pups born, 6 BAC transgenic pups were identified by PCR amplification across the SP6 and T7 vector-insert boundaries and by the presence of a *Bse*YI (New England BioLabs) restriction site (ss60981659; 5′-C*CCAGC-3′). Germline transmission and good breeding performance were established in 1 line.

In Vitro Electrophysiology. *Myk*/+ and +/+ mice (14–16 weeks old) were decapitated under isoflurane anesthesia and their brains isolated in ice-cold artificial cerebrospinal fluid (aCSF) containing (in mM): 124 NaCl, 26 $NaHCO_3$,

3 KCl, 2 $CaCl_2$, 2 $MgCl_2$, 26 $NaHCO_3$, 1.2 NaH_2PO_4, and 10 glucose. For experiments employing hippocampal slices, whole hippocampi were isolated, sliced at 400 μm on a manual chopper (Stoelting), and maintained as described previously (30). Methods for studies of in vitro epilepsy are described in the *SI Text*.

Magnetic Resonance Imaging. Magnetic resonance imaging was conducted as described previously (31).

Electron Microscopy. Electron microscopy was conducted as described previously (32).

Na^+,K^+-ATPase Functional Assays of Brain Homogenates. Brain tissue was homogenized in a buffer containing 85 mM NaCl, 20 mM KCl, 4 mM $MgCl_2$, 0.2 mM EGTA, 30 mM histidine (pH 7.2), and 10% sucrose (wt/vol), and was further permeabilized by incubation with 0.65 mg sodium deoxycholate/mL at a total brain protein concentration of 0.3 mg/mL in the presence of 2 mM EDTA and 2 mM imidazole at 20°C. The ouabain sensitive Na^+- and K^+-activated ATP hydrolysis rate was determined at 37°C by a colorimetric assay for liberated P_i (15). The deoxycholate treated brain tissue homogenate (25 μL) was added to 500 μL ATPase buffer containing 30 mM histidine (pH 7.5), 140 mM NaCl, 20 mM KCl, 3 mM $MgCl_2$, and 1 mM EGTA, and was allowed to react for 5 min with 3 mM ATP in the presence and absence of 3 mM ouabain. When the Na^+ concentration was varied, the K^+ concentration was kept at 20 mM, and when the K^+ concentration was varied, the Na^+ concentration was kept at 40 mM. The Na^+,K^+-ATPase active site concentration was determined by phosphorylation at 0°C in the presence of 2 μM [γ-^{32}P]ATP, 20 mM Tris (pH 7.5), 3 mM $MgCl_2$, 150 mM NaCl, 1 mM EGTA, and oligomycin (20 μg/mL) to inhibit dephosphorylation, and the catalytic turnover rate was calculated as the ratio between the ATPase activity and the active site concentration. In some experiments, the phosphorylation level was also determined at higher Mg^{2+} concentrations but under otherwise similar conditions. The phosphoenzyme was quantified using the Packard Cyclone storage phosphor system after acid quenching, washing by centrifugation and SDS-polyacrylamide gel electrophoresis at pH 6.0. The background phosphorylation determined in the presence of 50 mM KCl without NaCl was subtracted.

Protein Extraction and Blot Analysis. Whole brain homogenates from *Myk/Myk*, *Myk/*+ and +/+ E18 fetuses and from 12-week-old *Myk/*+, +/+ and *Myk/*+/BAC mice were subjected to SDS/PAGE followed by blotting and visualization with goat anti-Na^+,K^+-ATPase α3 (sc-16052; Santa Cruz; 1:100) or rabbit anti-NR1 (06–311; Upstate; 1:1,000). Immune complexes were detected by chemiluminescence (ECL Western blotting detection reagents, GE Healthcare). Plasma membrane and ER fractions of COS-1 cells transiently expressing transfected WT and mutant Na^+,K^+-ATPase were isolated by differential centrifugation according to procedures described previously (15, 33), and subjected to SDS/PAGE followed by blotting and visualization with anti-Na^+,K^+-ATPase α3 mouse monoclonal primary antibody (A-273; Sigma) and HRP-conjugated goat anti-mouse IgG secondary antibody.

Immunocytochemistry. Neocortical neuron cultures were prepared from E18 embryos, as described previously (34), and subjected to immunostaining with rabbit anti-Na^+/K^+-ATPase α3 (06–172; Upstate; 1:1,000) or mouse anti-agrin (AGR-131; Novus; 1:500) primary antibodies.

ACKNOWLEDGMENTS. We thank I. Vukobradovic, E. Weiss, J. Georgiou, and K. Lykke Pedersen for technical assistance; C. Snead and S. Cordes for advice; J. Lingrel for the provision of *Atp1a3*$^{tm1Ling/+}$ mice; and P. Carlen for critical reading of the manuscript. This work was supported by grants-in-aid to J.C.R. from the Canadian Institutes of Health Research (MOP 94856), and to B.V. from the Lundbeck Foundation, the Novo Nordisk Foundation (Fabrikant Vilhelm Pedersen og Hustrus Legat), the Danish Medical Research Council, and the Danish National Research Foundation (PUMPKIN Centre). J.C.R. holds a Canada Research Chair. S.J.C. held a Postdoctoral Fellowship from the Royal Society of London. J.T.H., S.D. and S.J.C. held Young Investigator Awards from the National Alliance for Research on Schizophrenia and Depression. J.P.L. was supported by a Canadian Institutes of Health Research fellowship.

1. Hauser WA, Hesdorffer DC (1990) in *Epilepsy*: *Frequency*, *Causes and Consequences* (Demos Press, New York).
2. Schmidt D, Löscher W (2005) Drug resistance in epilepsy: Putative neurobiologic and clinical mechanisms. *Epilepsia* 46:858–877.
3. Grisar T, Guillaume D, Delgado-Escueta AV (1992) Contribution of Na^+,K^+-ATPase to focal epilepsy: A brief review. *Epilepsy Res* 12:141–149.
4. Haglund MM, Schwartzkroin PA (1990) Role of Na-K pump potassium regulation and IPSPs in seizures and spreading depression in immature rabbit hippocampal slices. *J Neurophysiol* 63:225–239.
5. Somjen GG (2002) Ion regulation in the brain: Implications for pathophysiology. *Neuroscientist* 8:254–267.
6. Pietrobon D (2005) Migraine: New molecular mechanisms. *Neuroscientist* 11:373–386.
7. Davidson DL, Tsukada Y, Barbeau A (1978) Ouabain induced seizures: Site of production and response to anticonvulsants. *Can J Neurol Sci* 5:405–411.
8. Xiong ZQ, Stringer JL (2000) Sodium pump activity, not glial spatial buffering, clears potassium after epileptiform activity induced in the dentate gyrus. *J Neurophysiol* 83:1443–1451.
9. Vaillend C, Mason SE, Cuttle MF, Alger BE (2002) Mechanisms of neuronal hyperexcitability caused by partial inhibition of Na^+-K^+-ATPases in the rat CA1 hippocampal region. *J Neurophysiol* 88:2963–2978.
10. Gallanti A, et al. (2008) A novel de novo nonsense mutation in ATP1A2 associated with sporadic hemiplegic migraine and epileptic seizures. *J Neurol Sci* 273:123–126.
11. McGrail KM, Phillips JM, Sweadner KJ (1991) Immunofluorescent localization of three Na,K-ATPase isozymes in the rat central nervous system: Both neurons and glia can express more than one Na,K-ATPase. *J Neurosci* 11:381–391.
12. Brashear A, et al. (2007) The phenotypic spectrum of rapid-onset dystonia-parkinsonism (RDP) and mutations in the ATP1A3 gene. *Brain* 130:828–835.
13. Rodacker V, Toustrup-Jensen M, Vilsen B (2006) Mutations Phe785Leu and Thr618Met in Na^+,K^+-ATPase, associated with familial rapid-onset dystonia parkinsonism, interfere with Na^+ interaction by distinct mechanisms. *J Biol Chem* 281:18539–18548.
14. Snead OC, Clapcote SJ, Roder JC, Boulianne GL (2006) Novel strategies for the development of animal models of refractory epilepsy. *Adv Neurol* 97:155–171.
15. Vilsen B (1992) Functional consequences of alteration to Pro^{328} and Leu^{332} located in the 4th transmembrane segment of the α-subunit of the rat kidney Na^+,K^+-ATPase. *FEBS Lett* 314:301–307.
16. Morth JP, et al. (2007) Crystal structure of the sodium-potassium pump. *Nature* 450:1043–1049.
17. Avoli M, et al. (2002) Network and pharmacological mechanisms leading to epileptiform synchronization in the limbic system in vitro. *Prog Neurobiol* 68:167–207.
18. Tancredi V, Hwa GG, Zona C, Brancati A, Avoli M (1990) Low magnesium epileptogenesis in the rat hippocampal slice: Electrophysiological and pharmacological features. *Brain Res* 511:280–290.
19. McNamara JO, Huang YZ, Leonard AS (2006) Molecular signaling mechanisms underlying epileptogenesis. *Sci STKE* 356:12.
20. Hilgenberg LG, Su H, Gu H, O'Dowd DK, Smith MA (2006) α3Na^+/K^+-ATPase is a neuronal receptor for agrin. *Cell* 125:359–369.
21. Moseley AE, et al. (2007) Deficiency in Na,K-ATPase α isoform genes alters spatial learning, motor activity, and anxiety in mice. *J Neurosci* 27:616–626.
22. Misawa H, et al. (2002) Identification of a monogenic locus (jams1) causing juvenile audiogenic seizures in mice. *J Neurosci* 22:10088–10093.
23. Yang Y, Frankel WN (2004) Genetic approaches to studying mouse models of human seizure disorders. *Adv Exp Med Biol* 548:1–11.
24. Ikeda K, et al. (2003) Degeneration of the amygdala/piriform cortex and enhanced fear/anxiety behaviors in sodium pump α2 subunit (Atp1a2)-deficient mice. *J Neurosci* 23:4667–4676.
25. Wang J, et al. (2003) Interaction of calcineurin and type-A GABA receptor gamma 2 subunits produces long-term depression at CA1 inhibitory synapses. *J Neurosci* 23:826–836.
26. Goodkin HP, Yeh JL, Kapur J (2005) Status epilepticus increases the intracellular accumulation of GABAA receptors. *J Neurosci* 25:5511–5520.
27. Price EM, Lingrel JB (1988) Structure-function relationships in the Na,K-ATPase alpha subunit: Site-directed mutagenesis of glutamine-111 to arginine and asparagine-122 to aspartic acid generates a ouabain-resistant enzyme. *Biochemistry* 27:8400–8408.
28. Cortez MA, McKerlie C, Snead OC (2001) A model of atypical absence seizures: EEG, pharmacology, and developmental characterization. *Neurology* 56:341–349.
29. Ralph-Williams RJ, Paulus MP, Zhuang X, Hen R, Geyer MA (2003) Valproate attenuates hyperactive and perseverative behaviors in mutant mice with a dysregulated dopamine system. *Biol Psychiatry* 53:352–359.
30. Duffy S, Labrie V, Roder JC (2008) D-serine augments NMDA-NR2B receptor-dependent hippocampal long-term depression and spatial reversal learning. *Neuropsychopharmacology* 33:1004–1018.
31. Clapcote SJ, et al. (2007) Behavioral phenotypes of Disc1 missense mutations in mice. *Neuron* 54:387–402.
32. Wood DD, et al. (2008) Myelin localization of peptidylarginine deiminases 2 and 4: Comparison of PAD2 and PAD4 activities. *Lab Invest* 88:354–364.
33. Maruyama K, MacLennan DH (1988) Mutation of aspartic acid-351, lysine-352, and lysine-515 alters the Ca^{2+} transport activity of the Ca^{2+}-ATPase expressed in COS-1 cells. *Proc Natl Acad Sci USA* 85:3314–3318.
34. Liao D, Scannevin RH, Huganir R (2001) Activation of silent synapses by rapid activity-dependent synaptic recruitment of AMPA receptors. *J Neurosci* 21:6008–6017.